AGU PUBLICATIONS

Geophysical Research Letters

RESEARCH LETTER
10.1002/2016GL069511

**Key Points:**
- SGLs are present 670 m asl on the grounded ice of an East Antarctic outlet glacier
- SGLs on the floating ice tongue disappear during peak surface air temperatures
- SGLs on the grounded ice drain into surface channels which reroute water across the glacier surface

**Supporting Information:**
- Supporting Information S1

**Correspondence to:**
E. S. Langley,
emily.langley@durham.ac.uk

**Citation:**
Langley, E. S., A. A. Leeson, C. R. Stokes, and S. S. R. Jamieson (2016), Seasonal evolution of supraglacial lakes on an East Antarctic outlet glacier, *Geophys. Res. Lett.*, *43*, doi:10.1002/2016GL069511.

Received 22 MAY 2016
Accepted 1 AUG 2016
Accepted article online 8 AUG 2016



# Seasonal evolution of supraglacial lakes on an East Antarctic outlet glacier

**Emily S. Langley[1], Amber A. Leeson[2], Chris R. Stokes[1], and Stewart S. R. Jamieson[1]**

[1]Department of Geography, Durham University, Durham, UK, [2]Lancaster Environment Centre/Data Science Institute, Lancaster University, Lancaster, UK

**Abstract** Supraglacial lakes are known to influence ice melt and ice flow on the Greenland ice sheet and potentially cause ice shelf disintegration on the Antarctic Peninsula. In East Antarctica, however, our understanding of their behavior and impact is more limited. Using >150 optical satellite images and meteorological records from 2000 to 2013, we provide the first multiyear analysis of lake evolution on Langhovde Glacier, Dronning Maud Land (69°11'S, 39°32'E). We mapped 7990 lakes and 855 surface channels up to 18.1 km inland (~670 m above sea level) from the grounding line and document three pathways of lake demise: (i) refreezing, (ii) drainage to the englacial/subglacial environment (on the floating ice), and (iii) overflow into surface channels (on both the floating and grounded ice). The parallels between these mechanisms, and those observed on Greenland and the Antarctic Peninsula, suggest that lakes may similarly affect rates and patterns of ice melt, ice flow, and ice shelf disintegration in East Antarctica.

## 1. Introduction

The filling and drainage of supraglacial lakes is a potentially important component of an ice sheet's response to climate change. Observations in Greenland [*Das et al.,* 2008; *Doyle et al.,* 2013] have shown that their drainage and the surface-to-bed transfer of meltwater can alter the effective pressure of the ice-bed interface [*Bartholomew et al.,* 2012] and generate transient periods of enhanced basal sliding [*Bartholomew et al.,* 2011]. To date, most research has focussed on lakes on the Greenland Ice Sheet (GrIS), where drainage events have been synchronous with transient acceleration, ice-sheet uplift, and horizontal displacement, followed by subsidence and deceleration once meltwater has been dispersed [*Zwally et al.,* 2002; *Das et al.,* 2008].

Surface lakes on floating ice have the potential to affect ice shelf stability. Ponded surface water that drains englacially can contribute to the rapid disintegration of ice shelves, leading to reduced buttressing and to dynamic thinning of ice inland [*Scambos et al.,* 2000; *Banwell et al.,* 2013]. On ice shelves, the elastic properties of the ice and the gravitational load of lakes can also induce fractures with geometry conducive to multiple lake drainages [*Banwell et al.,* 2013; *Banwell and Macayeal*, 2015].

Despite the importance of lakes to ice-sheet and ice-shelf dynamics, research on their evolution in Antarctica has mostly been focussed on the Antarctic Peninsula (AP) [*Scambos et al.,* 2000] where rapid atmospheric and ocean warming has been observed in recent years. East Antarctica has long been considered insensitive to ocean-climate warming; however, recent models have predicted ice shelf collapse along its margin in the next century, possibly induced by supraglacial melt [*DeConto and Pollard,* 2016]. Variability in the intensity and duration of supraglacial melting has been linked to temporal variations in air temperature [*Trusel et al.,* 2012; *Liston and Winther,* 2005], suggesting a potential increase in melting as the climate warms. Meltwater has been documented ponding in lakes and channels near the grounding line of the Nivlisen Ice Shelf, Dronning Maud Land [*Kingslake et al.,* 2015], the Amery Ice Shelf [*Fricker et al.,* 2009], and along the Pacific Coast in Wilkes Land [*Miles et al.,* 2013]; however, a detailed multiyear study of supraglacial lake evolution in East Antarctica is currently lacking. Here we present the first quantitative multiyear data set of lake evolution and distribution on an East Antarctic outlet glacier for the period between 2000 and 2013.

## 2. Data and Methods

Langhovde is a 3 km wide glacier (Figure 1) that drains into Lützow-Holm Bay on the Soya Coast of East Antarctica (69°S, 39°E). The lower 10 km of the glacier flows in a channel confined by bedrock to the west and relatively slow moving ice to the east [*Sugiyama et al.,* 2014]. Surface velocities exceed 100 m $a^{-1}$ within 10 km of the terminus [*Fukuda et al.,* 2014], discharging ice into the ocean via a short (~1.6 to 3.3 km) ice shelf.

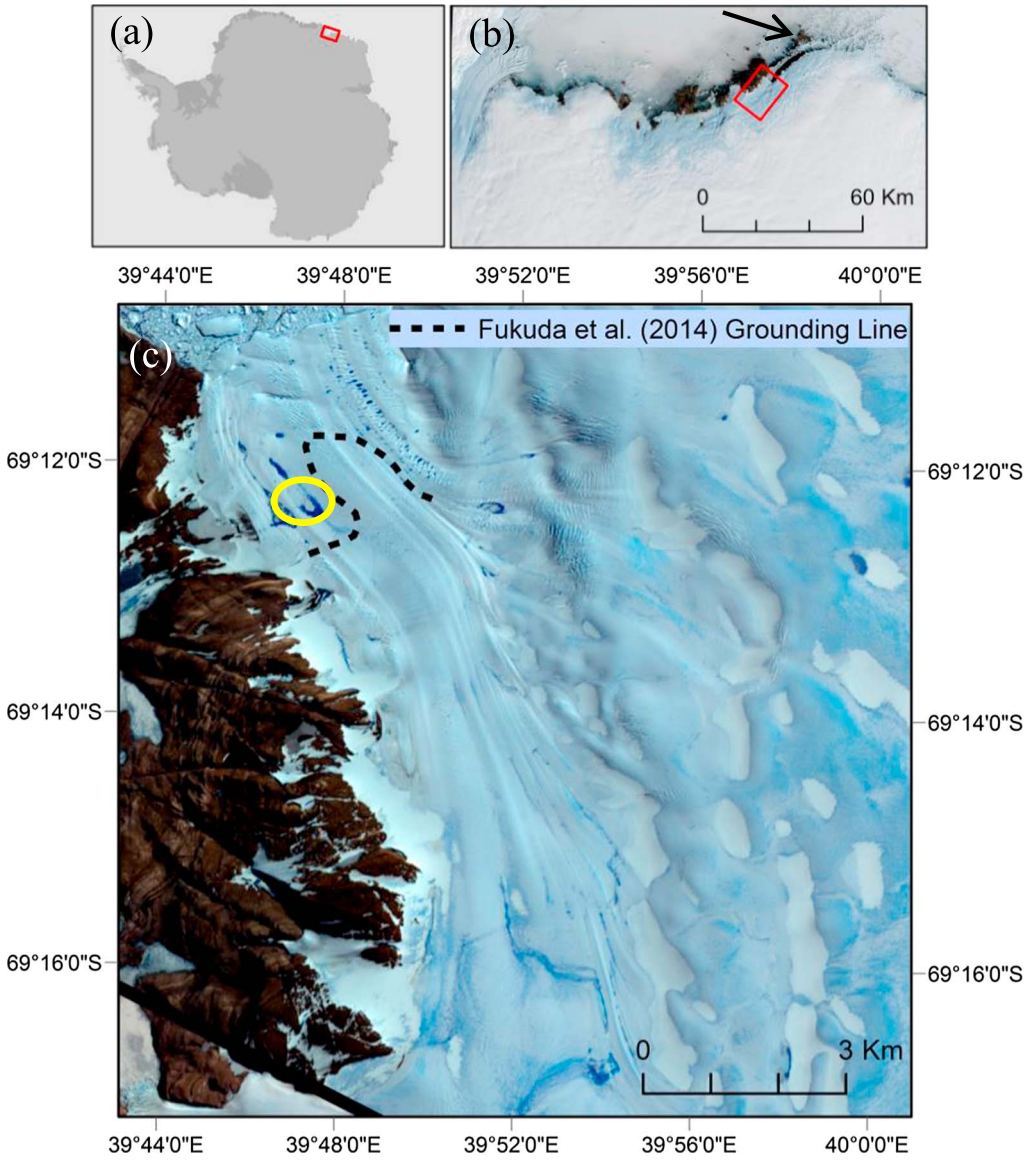


**Figure 1.** (a) Location of Soya Coast, Dronning Maud Land (red box) and (b) Landsat 7 image (15 January 2000) of Soya Coast with Langhovde Glacier (red box). Black arrow points to East Ongul island where Syowa Research Station is located. (c) ASTER image (4 January 2013) of Langhovde Glacier, showing the approximate location of the grounding line [*Fukuda et al.*, 2014]. Yellow circle refers to the supraglacial lake that is shown in Figure S2.

We acquired and georeferenced all cloud-free ASTER (Advanced Spaceborne Thermal Emission and Reflection Radiometer) and Landsat 7 ETM+ (Enhanced Thematic Mapper Plus) images of Langhovde Glacier for the austral summers (November to February) of 2000–2013 ($n = 153$). Landsat 7 images were pan-sharpened to the spatial resolution of the ASTER imagery (15 m). The temporal resolution of useable imagery was highest (~13 days) during the ablation seasons of 2007/2008, 2009/2010, 2010/2011, 2011/2012, and 2012/2013, enabling detailed observations during these years. No cloud-free images were available for 2003/2004.

A number of automated approaches for lake digitization [e.g., *Selmes et al.*, 2011; *Sundal et al.*, 2009] were tested, but generated errors when compared to manual methods [cf. *Leeson et al.*, 2013]. Therefore, meltwater features were digitized manually using multiple band combinations and standard image enhancement procedures (histogram equalization and contrast stretching) [*Glasser and Scambos*, 2008; *Lampkin and VanderBerg*, 2011]. The total number of lakes ($N_{total}$), total lake area ($A_{total}$), and mean lake area

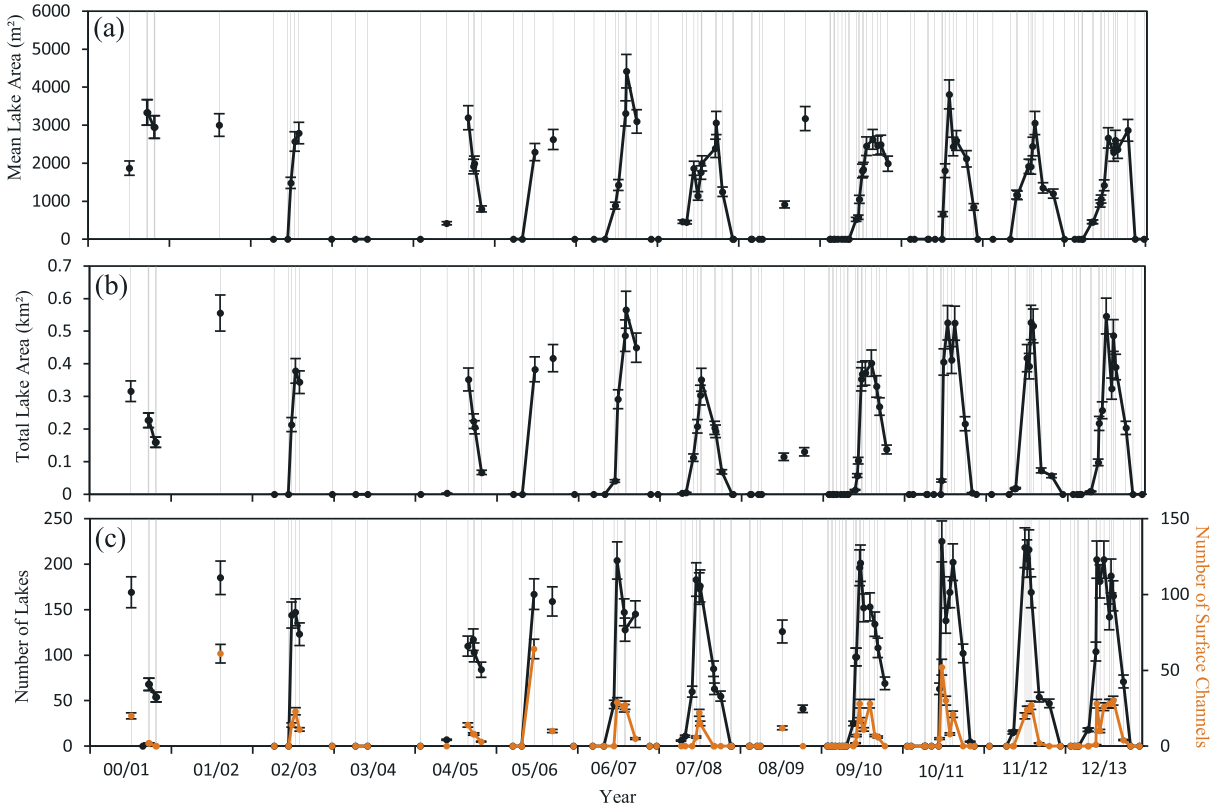


**Figure 2.** Supraglacial lake evolution from 2000 to 2013: (a) mean lake area, (b) total lake area, and (c) number of lakes and surface channels. Lines join dots (observations) that are less than 30 days apart. Grey vertical lines represent at least one cloud-free observation. Error was calculated by redigitizing 10 lakes (of varying size) in both an ASTER and Landsat 7 image (±10%).

($A_{mean}$) were measured in each image. Potential lakes $<450\,m^2$ (2 pixels in area) were omitted to minimize the possibility of false positives. Linear features identified as surface channels were digitized and their total number ($C_{total}$) recorded.

Lake depths were estimated using Landsat 7 band 3 and ASTER band 2 images [*Pope*, 2016]. We processed scaled radiance values to reflectance and then applied a radiative transfer model to each image to retrieve depth (see supporting information). The maximum, minimum, and mean of the maximum estimated lake depths found in each image were recorded.

We use the grounding line position of 1999–2003 from previous work [*Fukuda et al.*, 2014] to differentiate between lakes on grounded and floating ice. Daily mean surface air temperature records were acquired from the Japanese Meteorological Agency from the Syowa research station (elevation of 18 m), 20 km south of Langhovde Glacier (Figure 1b). We calculated the number of positive degree days for each ablation season by counting the number of days that experienced a mean surface air temperature >0°C.

## 3. Results

### 3.1. Annual and Interannual Variability

We mapped 7990 lakes and 855 surface channels over the 13 year period (Figure 2). Lakes form rapidly in late November, reaching their peak in number ($N_{total}$), area ($A_{total}$), and depth between late December and mid-January, and then decline at a slower rate (Figures 3 and 4). However, during peak summer (end of December/early January) it was not unusual to observe fluctuations in $N_{total}$, $A_{total}$, and $A_{mean}$ due to surface air temperature fluctuations (e.g., 2010/2011 and 2012/2013). Channels form later in the melt season (Figure 2c) and are rarely observed in November imagery, instead initiating between early December and mid-December, after lake formation. Channels also disappeared earlier in the season compared to lakes, with no channels observed in February (Figure 2c).

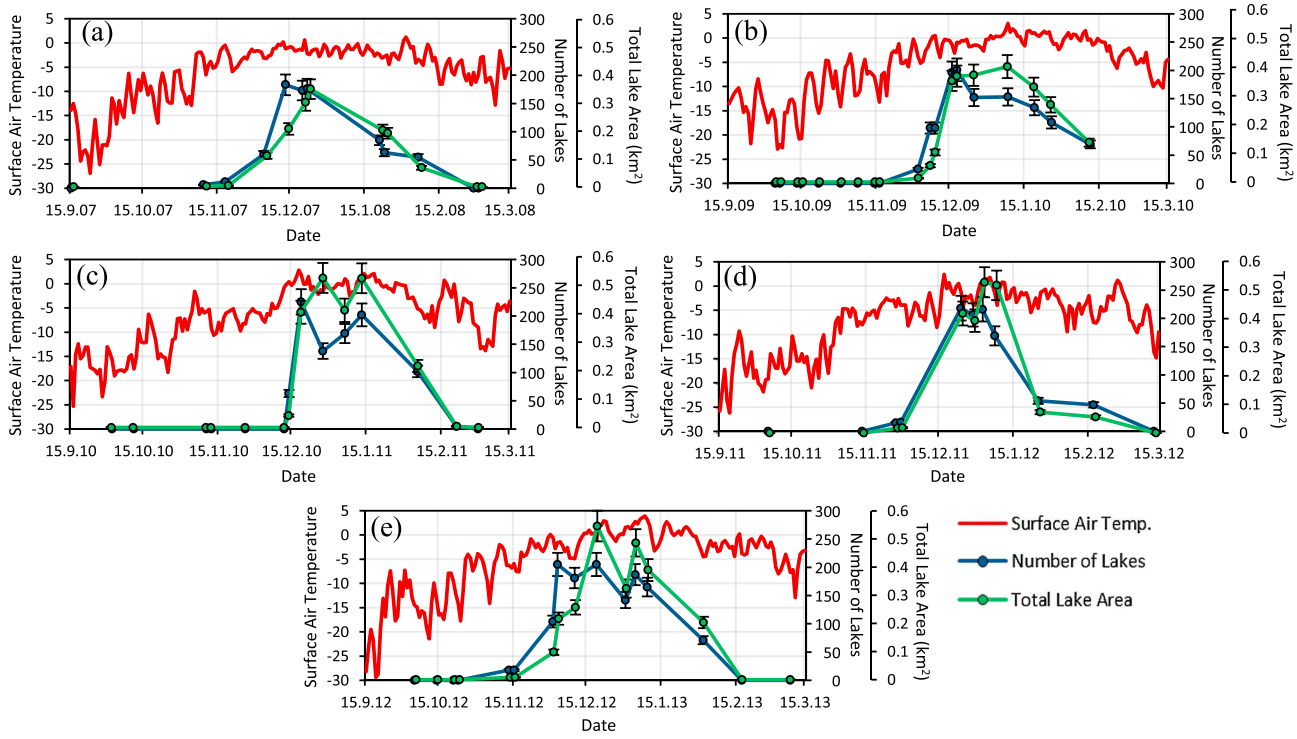


**Figure 3.** Annual variations in daily mean air surface temperatures, total lake area, and number of lakes. Years 2007/2008, 2009/2010, 2010/2011, 2011/2012, and 2012/2013 are displayed from the 13 year series due to their high temporal resolution. Note the strong coupling between total lake area and number of lakes and the response of lakes to fluctuations in daily mean surface air temperature.

Although the temporal pattern of lake and channel evolution is broadly the same for each austral summer, the absolute values of $N_{total}$, $A_{total}$, $A_{mean}$, and $C_{total}$ differ between years according to mean surface air temperature (see Figure S1 in the supporting information).

The warmest summer over the 13 year period was 2012/2013 (Figure 3e), with 37 positive degree days and a mean daily surface air temperature of 0.8°C in January. In comparison, 2007/2008 (Figure 3a) had only five positive degree days and a mean daily surface air temperature of −1.8°C in January. 2012/2013 produced significantly greater $A_{total}$ (55.7%) and $N_{total}$ (12%) compared to 2007/2008. Langhovde's glacier surface was characterized by 36% more surface channels, and six lakes were observed to overspill.

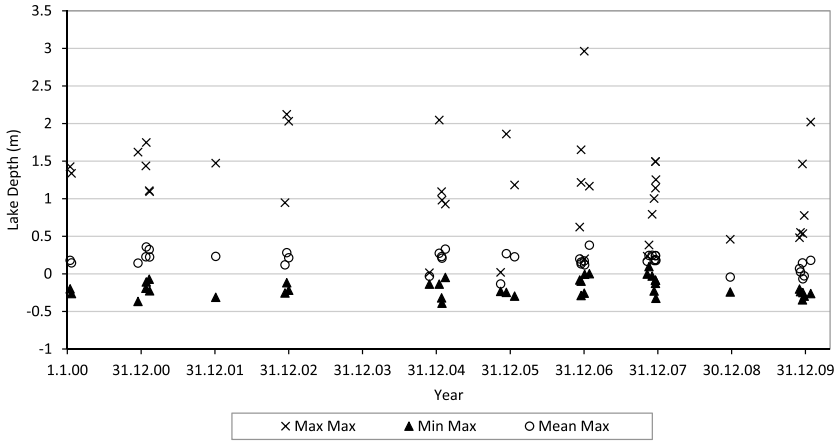


**Figure 4.** Interannual variation in the maximum-, minimum-, and mean-maximum lake depths per timeslice. For each image, the maximum lake depth was used because the mean depth is skewed by area. Error associated with lake depth is 24.5%.

Mean maximum lake depths evolve seasonally in line with lake area (Figure 4) and the deepest (3 m) lake occurred on 2 January 2007, coinciding with a maximum in lake area (Figure 3). Throughout the time series, area and depth peak at similar times, but over the 13 year time period there is no discernible trend in lake depth evolution. Analysis of an individual lake (Figure S2) indicates that there is no significant lag between the attainment of maximum lake area and maximum lake depth.

### 3.2. Geometry and Distribution of Lakes and Channels

The location of lakes on Langhovde Glacier is closely related to ice surface topography, with lake growth favoring low surface gradients. Lakes were found across the lower 18.1 km of the glacier, and range in elevation from 7 m above sea level (asl) on the ice shelf to 670 m asl up glacier (Figure S3). Each year, approximately 85% of lakes are present below 100 m asl, and 10% above 380 m asl, with an area in between that, is almost devoid of lakes due to the steeper surface slope.

There are two distinct populations of lakes: those that persistently occupy the same depressions each year and those that are more transient. Lakes that reoccur in the same basins are found on the grounded part of Langhovde Glacier (Figure S3a). They are the largest lakes we observe, reaching a maximum of 166,852 $m^2$ in area. In comparison, transient lakes are observed on the floating ice shelf and appear in different locations each year (Figure S3b). They are much smaller than those observed at higher elevations, rarely exceeding 17,000 $m^2$ in area. They often form in depressions that lie between flow stripes on the surface, as well as accumulating in major crevasses. They are observed overspilling and coalescing into larger drainage networks during high-melt years (i.e., 2012/2013). Close to the grounding line (Figure S3b), lakes show a combination of these characteristics. They initiate from the same locations each year but advect and elongate with ice flow over our observation period.

Linear surface channels are observed every austral summer (Figure S4). The majority of channels are located on the grounded ice and tend to follow the same path each year, initiating from, and terminating at, the same point. They are found up to 15 km inland (630 m asl) and reach lengths of 3.5 km. Some initiate from lakes and form sinuous drainage networks, following the local topographic slope. Although these channels are fed by lakes, we never observe lakes fully emptying via a channel.

### 3.3. Lake Shrinkage and Disappearance

Towards the end of the austral summer, many lake surfaces refreeze from the center outward (Figures 5a and 5b). This process is first observed at higher elevations and spreads to lower elevations. For most lakes, this is their predominant fate at the end of the ablation season. However, our observations reveal another mechanism through which lakes shrink, or even disappear, on the floating ice shelf. During peak melt, some lakes on the ice shelf are observed shrinking from the outside in, rather than the center outward, suggesting through-ice drainage (Figures 5c and 5d). This behavior occurs when mean daily surface air temperatures are $>0$°C. For example, between 4 January 2013 and 9 January 2013, when the mean surface air temperature was 3.2°C in the lower reaches of the glacier, 21 lakes shrunk (11% of total number of lakes), despite other lakes growing in the same area (Figure S5a). The timeframe over which these drainage events take place is difficult to discern due to the temporal resolution of our imagery. We do not only observe slow drainage (Figure S5a) but also observe a lake draining fully in less than 5 days (Figure S5b). We also note an unusual concentric fracture surrounding a former lake in 2010 in a high-resolution (~0.5 m) DigitalGlobe image (Figure 5e). The feature is $230 \times 170$ m and is divided into two sections. The center appears at a different elevation to the surrounding section (either lower or higher). The entire feature is encircled by a fracture, which is filled with meltwater being fed by a channel.

## 4. Discussion

### 4.1. Seasonal Evolution of Lakes

Similar to studies on the GrIS [*McMillan et al.,* 2007; *Johansson et al.*, 2013; *Sundal et al.,* 2009] and in Dronning Maud Land [*Trusel et al.,* 2012], Langhovde Glacier shows strong annual and interannual variation in $N_{total}$, $A_{total}$, $A_{mean}$, and lake depth (Figures 3 and 4). Unsurprisingly, there is a strong correlation between supraglacial melt and surface air temperature (Figure S1), which determines the amount of energy available for melt each year [*Bartholomew et al.,* 2010]. Lake initiation and evolution is directly correlated with surface air temperature and, more specifically, the number of positive degree days [*Zwally et al.,* 2002; *Joughin et al.,* 2008].

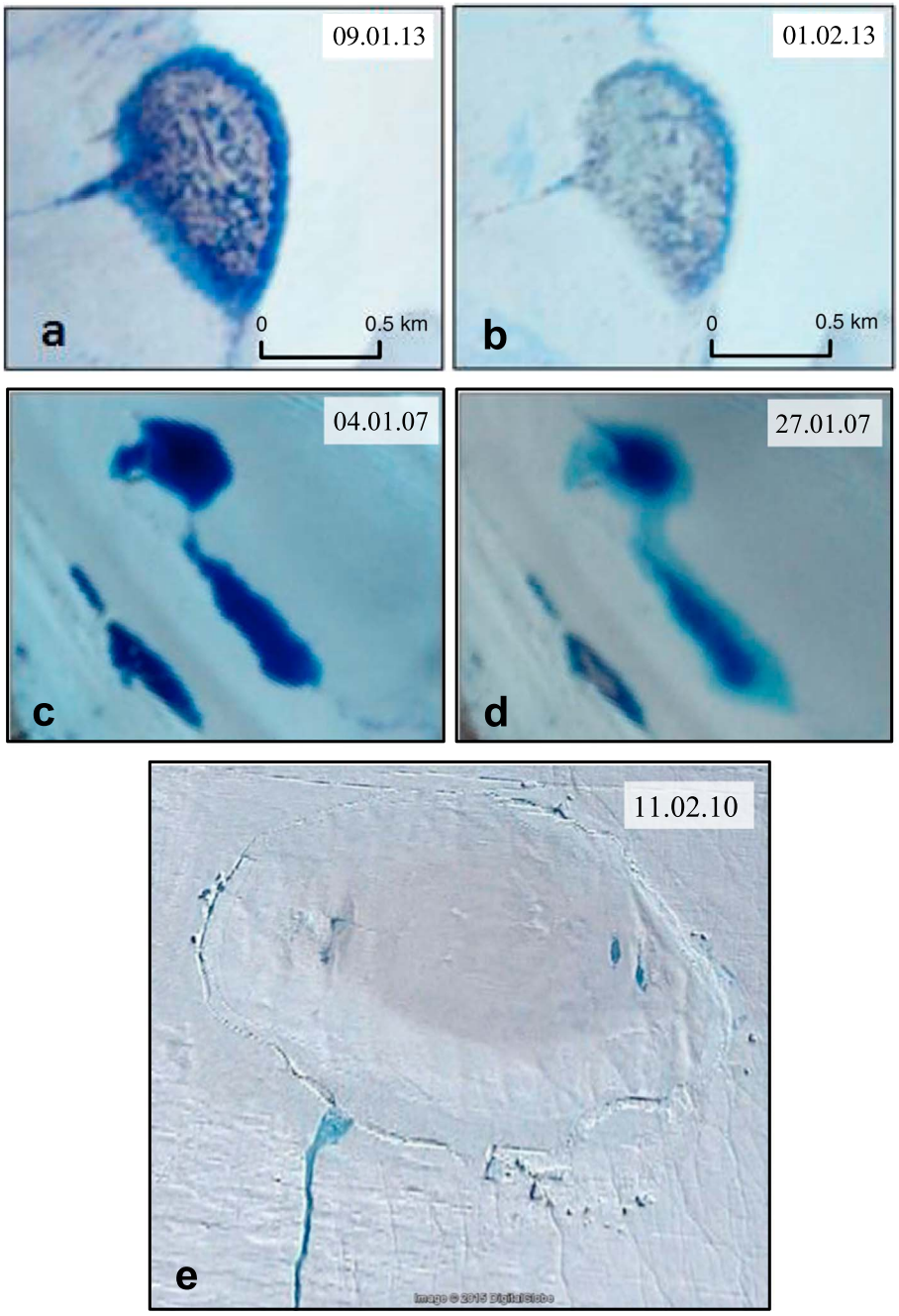


**Figure 5.** Examples of lake behavior on Langhovde Glacier from ASTER imagery. (a and b) A lake located on the grounded ice refreezing at the end of the austral summer, characterized by floating ice in the center that gradually spreads outwards. (c and d) Lakes located on the floating ice shelf, close to the grounding line, shrinking midseason. (e) A DigitalGlobe image (Google Earth) from 2010 identifies an unusual fracture on the floating ice shelf, developed from a former lake.

Once lakes and channels appear, their evolution is highly sensitive to surface air temperature increases (Figure S1), a very small increase in the average daily surface air temperature can lead to a relatively large increase in the $N_{total}$, $A_{total}$, $A_{mean}$, $C_{total}$, and lake depth. This has been noted in previous work [*Kingslake et al.,* 2015] and likely explains why lake growth at the beginning of the melt season is generally very rapid (a few weeks: Figure 3). A number of location-specific factors and feedback mechanisms have been proposed to explain the sensitivity of lakes and channels to surface air temperatures [*Bartholomew et al.,* 2010]. For example, in Dronning Maud Land, an abundancy of bedrock outcrops and blue-ice regions are likely to be

important in maintaining microclimatic temperatures and absorbing solar radiation, thereby enhancing surface melt [*Liston and Winther*, 2005]. Furthermore, the reduced albedo over a lake favors melting at a rate greater than that of surface air temperature increase [*Lüthje et al.,* 2006]. This, alongside lake-bottom ablation, which involves greater melting at the base and sides of a lake due to the higher thermal conductivity of water, are plausible reasons for the sensitivity of lakes to surface air temperatures [*Box and Ski*, 2007; *Tedesco et al*., 2012].

### 4.2. Lakes and Channels on Grounded Ice

Similar to surface lakes described on the GrIS, lakes that occupy the same depressions each year on the grounded ice of Langhovde Glacier are likely a reflection of the interaction between subglacial topography and ice flow [*Echelmeyer et al.,* 1991; *Sergienko*, 2013]. Alongside climate forcing, internal processes (e.g., ice-flow physics and bedrock features) determine the distribution, geometry, and volume of lakes [*Banwell et al.,* 2014]. We observe lakes refreezing on the grounded ice, which has the potential to affect surface energy balance. Lakes that refreeze, releasing latent heat, at the end of the ablation season may influence temperature distribution and thermodynamics in the upper layers of the ice [*Tedesco et al.,* 2012]. Refreezing of water can modify the snowpack energy budget, morphology, density, and isotopic signature [*Cuffey and Paterson*, 2010].

The majority of supraglacial channels were above the grounding line. Surface channels have been observed elsewhere in East Antarctica, specifically the Nivlisen ice shelf [*Kingslake et al.,* 2015], but they have rarely been documented on the grounded ice sheet. Sinuous channels that we observed instigating from lakes closely resemble those described by *Kingslake et al.* [2015], and we assume a similar initiation mechanism via the turbulent dissipation of heat [*Tedesco and Steiner,* 2011]. The delay in channel formation (Figures 2c and S1b) is probably related to the time it takes for a lake to fill and overspill its boundaries. We observe "stable drainage," where channel incision, and lake water-level drawdown, does not exceed meltwater input and so does not entirely drain the lake. Because "unstable drainage" is considered a product of greater initial lake area and input [*Kingslake et al*., 2015], such events might be observed on Langhovde Glacier in the near future, should warming occur.

The presence of surface channels can also have an important impact on ice-sheet dynamics. As documented in Greenland, channels can connect lakes to moulins on the glacier surface, thereby supplying water to the ice/bed interface [*Das et al*., 2008; *Tedesco et al*., 2013]. Although the resolution of imagery in this study was not sufficient to identify moulins on the glacier surface, we note that channels often terminated in consistent locations throughout the melt season (Figure S4). However, some of the linear features interpreted as channels, located on the grounded part of the glacier, did not initiate from a lake (Figure S4). Their static nature and consistency in length and position suggest they are instead thin lakes similar to those described by *Glasser and Scambos* [2008] on the Larsen B ice shelf.

### 4.3. Lakes on Floating Ice and Their Drainage

Lakes observed on the floating ice shelf tend to develop in surface crevasses [*McGrath et al.,* 2012]. We suggest that the flexure and fracturing of the floating ice assists the development of ice-surface depressions in which meltwater can pond [e.g., *MacAyeal and Sergienko*, 2013].

Vertical lake drainage has not previously been reported on floating ice in East Antarctica, but our observations reveal a number of occasions where lakes have apparently disappeared in this manner (Figures S5a and S5b). The quickest we observe a lake fully draining is 5 days (Figure S5b); this is slower than on the GrIS and AP [*Banwell et al.,* 2013]. On the GrIS for example, "slow-draining lakes" are defined as those draining in less than 2 days but more than a few hours [*Tedesco et al.,* 2013]. It is therefore not clear whether lake drainage via hydrofracture takes place. Nonetheless, we observed a circular feature in higher-resolution imagery (Figure 5e), which shows similarities to ice dolines described on the Larsen B and Amery ice shelves [*Bindschadler et al.,* 2002; *Fricker et al.,* 2002]. These oval-shaped depressions have been observed on ice shelves, where hydraulic connections between lakes and the underlying ocean have been made [*Glasser and Scambos*, 2008].

Further research could usefully focus on confirming that lakes are able to drain to the subshelf ocean (and not just englacially) and examine their impact on ice shelf stability. We find that warmer ablation seasons are characterized by more lakes of a larger area (Figures 3 and S1a). Since larger lakes are considered more prone

to hydrofracturing and therefore lake drainage [*Krawczynski et al.,* 2009], more fast lake drainage events are predicted on Langhovde Glacier if the coast of Dronning Maud Land experiences higher ablation as the climate warms.

## 5. Conclusions

We report the first quantitative multiyear study of supraglacial lake evolution above and below the grounding line of an East Antarctic outlet glacier, documenting annual and interannual variability in the total number, area, and depth of lakes and the total number of surface channels, which is strongly linked to surface air temperatures. We show lakes existing up to 670 m asl (18 km) inland, the highest so far reported in East Antarctica. Our results suggest that at the end of their life, lakes either (i) refreeze, (ii) drain vertically through the ice or (iii) drain laterally via surface channels. However, the mechanism by which vertical drainage is achieved (partial drainage or hydrofracture) is not clear. Nonetheless, we suggest similar lake and channel populations are likely to exist on other outlet glaciers and that they are a potentially important, but hitherto overlooked, component of outlet glacier dynamics in East Antarctica.

**Acknowledgments**

Data generated for this paper are available from the corresponding author. S.S. R.J. was supported by Natural Environment Research Council (NERC) Fellowship NE/J018333/1. We thank climate scientists at the National Institute of Polar Research for access to Syowa temperature data. This manuscript was considerably improved by constructive comments from two anonymous reviewers and the Editor (Julienne Stroeve).

## References

Banwell, A. F., and D. R. Macayeal (2015), Ice-shelf fracture due to viscoelastic flexure stress induced by fill/drain cycles of supraglacial lakes, *Antarct. Sci.*, *27*(06), 587–597.

Banwell, A. F., D. R. MacAyeal, and O. V. Sergienko (2013), Breakup of the Larsen B Ice Shelf triggered by chain reaction drainage of supraglacial lakes, *Geophys. Res. Lett.*, *40*, 5872–5876, doi:10.1002/2013GL057694.

Banwell, A. F., M. Caballero, N. S. Arnold, N. F. Glasser, L. M. Cathles, and D. R. MacAyeal (2014), Supraglacial lakes on the Larsen B ice shelf, Antarctica, and at Paakitsoq, West Greenland: A comparative study, *Ann. Glaciol.*, *55*(66), 1–8.

Bartholomew, I., P. Nienow, D. Mair, A. Hubbard, M. A. King, and A. Sole (2010), Seasonal evolution of subglacial drainage and acceleration in a Greenland outlet glacier, *Nat. Geosci.*, *3*(6), 408–411.

Bartholomew, I., P. Nienow, A. Sole, D. Mair, T. Cowton, S. Palmer, and J. Wadham (2011), Supraglacial forcing of subglacial drainage in the ablation zone of the Greenland ice sheet, *Geophys. Res. Lett.*, *38*, L08502, doi:10.1029/2011GL047063.

Bartholomew, I., P. Nienow, A. Sole, D. Mair, T. Cowton, and M. A. King (2012), Short-term variability in Greenland Ice Sheet motion forced by time-varying meltwater drainage: Implications for the relationship between subglacial drainage system behavior and ice velocity, *J. Geophys. Res.*, *117*, F03002, doi:10.1029/2011JF002220.

Bindschadler, R., T. A. Scambos, H. Rott, P. Skvarca, and P. Vornberger (2002), Ice dolines on Larsen Ice Shelf, Antarctica, *Ann. Glaciol.*, *34*(1), 283–290.

Box, J. E., and K. Ski (2007), Remote sounding of Greenland supraglacial melt lakes: Implications for subglacial hydraulics, *J. Glaciol.*, *53*(181), 257–265.

Cuffey, K. M., and W. S. B. Paterson (2010), *The Physics of Glaciers*, 4th ed., Butterworth-Heinemann, Burlington, Mass.

Das, S. B., I. Joughin, M. D. Behn, I. M. Howat, M. A. King, D. Lizarralde, and M. P. Bhatia (2008), Fracture propagation to the base of the Greenland ice sheet during supraglacial lake drainage, *Science*, *320*(5877), 778–781.

DeConto, R. M., and D. Pollard (2016), Contribution of Antarctica to past and future sea-level rise, *Nature*, *531*(7596), 591–597.

Doyle, S. H., A. L. Hubbard, C. F. Dow, G. A. Jones, A. Fitzpatrick, A. Gusmeroli, B. Kulessa, K. Lindback, R. Pettersson, and J. E. Box (2013), Ice tectonic deformation during the rapid in situ drainage of a supraglacial lake on the Greenland Ice Sheet, *Cryosphere*, *7*, 129–140.

Echelmeyer, K., T. Clarke, and W. Harrison (1991), Surficial glaciology of Jakobshavns Isbræ, West Greenland: Part I. Surface morphology, *J. Glaciol.*, *37*(127), 368–382.

Fricker, H. A., I. Allison, M. Craven, G. Hyland, A. Ruddell, N. Young, R. Coleman, M. King, K. Krebs, and S. Popov (2002), Redefinition of the Amery Ice Shelf, East Antarctica, grounding zone, *J. Geophys. Res.*, *107*(B5), 2092, doi:10.1029/2001JB000383.

Fricker, H. A., R. Coleman, L. Padman, T. A. Scambos, J. Bohlander, and K. M. Brunt (2009), Mapping the grounding zone of the Amery Ice Shelf, East Antarctica using InSAR, MODIS and ICESat, *Antarct. Sci.*, *21*(05), 515–532.

Fukuda, T., S. Sugiyama, T. Sawagaki, and K. Nakamura (2014), Recent variations in the terminus position, ice velocity and surface elevation of Langhovde Glacier, East Antarctica, *Antarct. Sci.*, *26*(06), 636–645.

Glasser, N. F., and T. A. Scambos (2008), A structural glaciological analysis of the 2002 Larsen Ice Shelf collapse, *J. Glaciol.*, *54*(184), 3–16.

Johansson, A. M., P. Jansson, and I. A. Brown (2013), Spatial and temporal variations in lakes on the Greenland Ice Sheet, *J. Hydrol.*, *476*, 314–320.

Joughin, I., S. B. Das, M. A. King, B. E. Smith, I. M. Howat, and T. Moon (2008), Seasonal speedup along the western flank of the Greenland Ice Sheet, *Science*, *320*(5877), 781–783.

Kingslake, J., F. Ng, and A. Sole (2015), Modelling channelized surface drainage of supraglacial lakes, *J. Glaciol.*, *61*(225), 185–199.

Krawczynski, M. J., M. D. Behn, S. B. Das, and I. Joughin (2009), Constraints on the lake volume required for hydro-fracture through ice sheets, *Geophys. Res. Lett.*, *36*, L10501, doi:10.1029/2008GL036765.

Lampkin, D. J., and J. VanderBerg (2011), A preliminary investigation of the influence of basal and surface topography on supraglacial lake distribution near Jakobshavn Isbrae, western Greenland, *Hydrol. Processes*, *25*(21), 3347–3355.

Leeson, A. A., A. Shepherd, A. V. Sundal, A. M. Johansson, N. Selmes, K. Briggs, A. E. Hogg, and X. Fettweis (2013), A comparison of supraglacial lake observations derived from MODIS imagery at the western margin of the Greenland ice sheet, *J. Glaciol.*, *59*(218), 1179–1188.

Liston, G. E., and J. G. Winther (2005), Antarctic surface and subsurface snow and ice melt fluxes, *J. Clim.*, *18*(10), 1469–1481.

Lüthje, M., L. T. Pedersen, N. Reeh, and W. Greuell (2006), Modelling the evolution of supraglacial lakes on the West Greenland ice-sheet margin, *J. Glaciol.*, *52*(179), 608–618.

MacAyeal, D. R., and O. V. Sergienko (2013), Flexural dynamics of melting ice shelves, *Ann. Glaciol.*, *54*(63), 1–10.

McGrath, D., K. Steffen, T. Scambos, H. Rajaram, G. Casassa, and J. L. Rodriguez Lagos (2012), Basal crevasses and associated surface crevassing on the Larsen C ice shelf, Antarctica, and their role in ice-shelf instability, *Ann. Glaciol.*, *53*(60), 10–18.

McMillan, M., P. Nienow, A. Shepherd, T. Benham, and A. Sole (2007), Seasonal evolution of supra-glacial lakes on the Greenland Ice Sheet, *Earth Planet. Sci. Lett.*, *262*(3), 484–492.
Miles, B. W. J., C. R. Stokes, A. Vieli, and N. J. Cox (2013), Rapid, climate-driven changes in outlet glaciers on the Pacific coast of East Antarctica, *Nature*, *500*(7464), 563–566.
Pope, A. (2016), Reproducibly estimating and evaluating supraglacial lake depth with Landsat 8 and other multispectral sensors, *Earth Space Sci.*, *3*(4), 176–188.
Scambos, T. A., C. Hulbe, M. Fahnestock, and J. Bohlander (2000), The link between climate warming and break-up of ice shelves in the Antarctic Peninsula, *J. Glaciol.*, *46*(154), 516–530.
Selmes, N., T. Murray, and T. D. James (2011), Fast draining lakes on the Greenland ice sheet, *Geophys. Res. Lett.*, *38*, L15501, doi:10.1029/2011GL047872.
Sergienko, O. V. (2013), Glaciological twins: Basally controlled subglacial and supraglacial lakes, *J. Glaciol.*, *59*(213), 3–8.
Sugiyama, S., T. Sawagaki, T. Fukuda, and S. Aoki (2014), Active water exchange and life near the grounding line of an Antarctic outlet glacier, *Earth Planet. Sci. Lett.*, *399*, 52–60.
Sundal, A. V., A. Shepherd, P. Nienow, S. Palmer, and P. Huybrechts (2009), Evolution of supraglacial lakes across the Greenland Ice Sheet, *Remote Sens. Environ.*, *113*, 2164–2171.
Tedesco, M., and N. Steiner (2011), In-situ multispectral and bathymetric measurements over a supraglacial lake in western Greenland using a remotely controlled watercraft, *Cryosphere*, *5*(2), 445–452.
Tedesco, M., M. Lüthje, K. Steffan, N. Steiner, X. Fettweise, I. Willis, N. Bayou, and A. Banwell (2012), Measurement and modelling of ablation of the bottom of supraglacial lakes in western Greenland, *Geophys. Res. Lett.*, *32*, L02502, doi:10.1029/2011GL049882.
Tedesco, M., I. C. Willis, M. J. Hoffman, A. F. Banwell, P. Alexander, and N. S. Arnold (2013), Ice dynamic response to two modes of surface lake drainage on the Greenland ice sheet, *Environ. Res. Lett.*, *8*(3), 034007.
Trusel, L. D., K. E. Frey, and S. B. Das (2012), Antarctic surface melting dynamics: Enhanced perspectives from radar scatterometer data, *J. Geophys. Res.*, *117*, F02023, doi:10.1029/2011JF002126.
Zwally, H. J., W. Abdalati, T. Herring, K. Larson, J. Saba, and K. Steffen (2002), Surface melt-induced acceleration of Greenland Ice Sheet flow, *Science*, *297*(5579), 218–222.